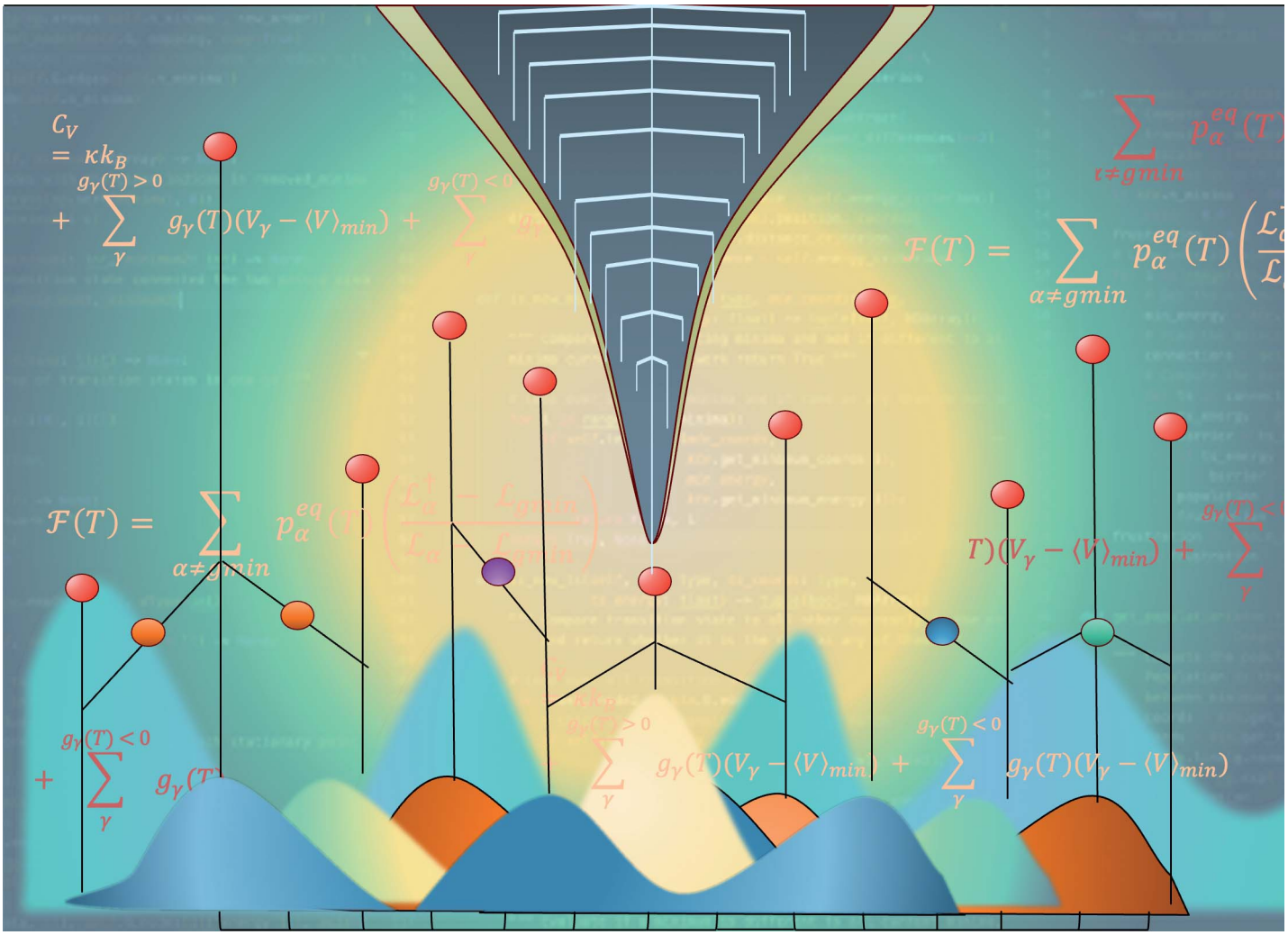

Showcasing research from the collaboration between the groups of Professor Wales - Yusuf Hamied, Department of Chemistry, University of Cambridge, and Dr Pyzer-Knapp - IBM Research Europe.

Insights into machine learning models from chemical physics: an energy landscapes approach (EL for ML)

This work showcases how principles from Chemical Physics, namely the Energy Landscapes approach, can be applied to machine learning models. We show how various physical properties find analogues in machine learning systems, and how these properties can be employed to both increase understanding of the machine learning 'black-box' and enhance the performance of machine learning models.

As featured in:

See Edward O. Pyzer-Knapp, David J. Wales *et al.*, *Digital Discovery*, 2024, **3**, 637.

ROYAL SOCIETY OF CHEMISTRY

rsc.li/digitaldiscovery

Registered charity number: 207890

Digital Discovery

ROYAL SOCIETY OF CHEMISTRY

TUTORIAL REVIEW

View Article Online
View Journal | View Issue

Cite this: *Digital Discovery*, 2024, **3**, 637

Insights into machine learning models from chemical physics: an energy landscapes approach (EL for ML)

Maximilian P. Niroomand, [a] Luke Dicks, [b] Edward O. Pyzer-Knapp *[b] and David J. Wales *[a]

Received 9th October 2023
Accepted 26th January 2024

DOI: 10.1039/d3dd00204g

rsc.li/digitaldiscovery

The study of energy landscapes as a conceptual framework, and a source of novel computational tools, is an active area of research in chemistry and physics. The energy landscape provides insight into structure, dynamics, and thermodynamics when combined with tools from statistical mechanics and unimolecular rate theory. This approach can also be applied to questions that arise in machine learning. Here, the loss landscape (LL) of a machine learning system is treated in the same way as the energy landscape for a molecular system. In this contribution we summarise and discuss applications of energy landscapes for machine learning (EL4ML). We will outline how various physical properties find analogues in machine learning systems, and show how these properties can be employed to both increase understanding of the machine learning 'black-box' and enhance the performance of machine learning models.

1 Introduction

In the physical sciences, energy landscapes[1] provide a computational framework to predict structure, thermodynamics, and dynamics.[2] Exploring the energy landscape means computing the potential energy E for a given atomic configuration, defined by the coordinates of the individual atoms in $\mathbb{R}^3$. The potential energy surface (PES) gives the energy for any combination of coordinates of the individual atoms. The PES is a continuous, non-convex function, in which local minima correspond to locally-stable states of the system, and potentially interesting configurations. The Murrell–Laidler theorem states that the lowest barrier between local minima involves a pathway mediated by index one saddle points (transition states).[3] These transition states are essential to describing the dynamics of a physical system. An illustrative PES is shown in Fig. 1, where the zero-gradient transition state separates two minima. The global minimum corresponds to the lowest potential energy achievable for a given system, which corresponds to the equilibrium state at low temperature.

In machine learning, the problem posed is analogous to optimising atomistic arrangements in molecular systems. Given a set of variables (weights, hyperparameters *etc.*), a loss function is minimised to provide the best possible solution to the problem. As for molecular systems, machine learning is an optimisation problem, with the aim to minimise the cost function and identify the lowest-lying solution. In a (supervised) machine learning system, this solution is the set of weights/hyperparameters describing an arbitrary function that best fits some input data to known outputs.

In ML there is an additional consideration, requiring a model generalising well to unseen data. For a given machine learning algorithm and some data, the loss landscape describes the quality of each possible weight/hyperparameter combination. Importantly, these models are only conditioned on the training data, hence the LL cannot make a statement about generalisation to unseen testing data. Numerous loss functions exist, from simple mean squared error losses to cross-entropy, contrastive, or approximate AUC loss functions. Thus, the correlation between loss value and performance of the minimum must be viewed with caution. The global minimum of the LL is the best guess as to which set of weights may be optimal for the specific problem, but optimality cannot be guaranteed. Train-test generalisability is not the focus of this contribution, but the reader should keep this issue in mind.

To characterise the loss landscape (LL) of a machine learning system, only the training data is relevant. Hence, the global minimum is the set of weights that minimise the loss (energy) for a given cost/loss function and training data. Note that this setup implies that, for a standard loss function, overfitting the model to training data is encouraged by the formulation of the problem. Thus, ideally, the model would perfectly predict the correct output for each input, irrespective of performance on unseen data. In Table 1, we have summarised the most important features to describe an energy landscape, and what they mean when translated to a ML setting.

[a]*University of Cambridge, Department of Chemistry, Cambridge, UK. E-mail: mpn26@cam.ac.uk; dw34@cam.ac.uk*

[b]*IBM Research UK, Daresbury, UK. E-mail: EPyzerK3@uk.ibm.com*

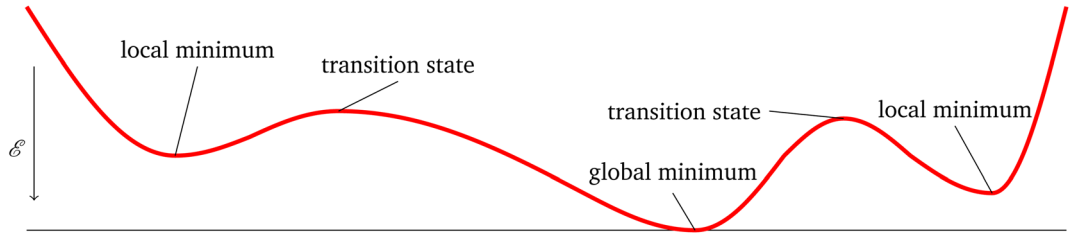

Fig. 1 A simplified potential energy landscape. Each value of the red line is the potential energy at a specific set of atom coordinates. Hence, the red line is an energy function f for some molecule.

Table 1 Comparison of energy landscapes features in molecular systems and their analogue in ML systems

Feature	Molecular PES	ML LL
Energy	Potential energy	Loss value
Temperature	Physical temperature	Fictitious parameter
Coordinates	Atomistic coordinates	Weights/hyperparameters
Local minimum	Locally-stable molecular isomer	Locally optimal weights
Global minimum	Energetically most favourable molecular isomer	Best weights for given loss function

2 Motivation: EL4ML

Machine learning has become one of the most active fields in science due to its impact across a broad range of applications. These applications range from games, such as chess,[4] Go,[5] or the collaborative Dota 2[6] to autonomous driving (covered extensively in ref. 7), protein structure prediction[8] mathematical proofs,[9] chat bots,[10,11] image generation[12,13] and many more. Applications to the physical sciences, including force-field parametrisation are discussed in ref. 14. This list is far from exhaustive, and novel machine learning models are developed and open-sourced every day. The basic foundation of the machine learning approach is that, given enough data and computational resources, the fitting and prediction problem is solvable in principle. In fact, it can be shown that, given enough parameters, any dataset can be fitted perfectly by a machine learning model.[15] However, we seek a deeper understanding of why and when machine learning works, and the fact that there exists a function to map given input to output does not provide understanding or interpretation of which features from the input lead the model to a given output choice.

Interpretability in ML has received increasing attention[16–18] with the realisation that in many fields, an understanding of why a certain prediction is being made, is as important as the accuracy. Unfortunately, interpreting a high-dimensional and complex function is difficult.[19] Recent efforts in interpretability have been summarised in Zhang *et al.*[16] Usually, these approaches revolve around understanding the gradients of the loss function with respect to the input, to understand how changes in the input affect the output, as in Davies *et al.*[9] However, given the relatively high complexity of machine learning models such as neural networks, this analysis is often insufficient and does not provide a complete picture.[19]

To better understand the foundations of machine learning capabilities, the loss landscapes of machine learning systems[20–22] can be analysed. For reasons of computational cost, it is common practice in machine learning to start from a given set of initial weights, chosen either randomly or by some initialisation scheme,[23] minimise the loss as far as possible with a greedy algorithm, and accept this result for the trained weights. Perhaps unexpectedly, this procedure seems to work well, and various explanations for this fortuitous situation have been suggested.[24,25] The most prominent suggestion derives from Goodfellow *et al.*[26] They report what they call the Monotonic Linear Interpolation (MLI) property, the fact that there usually exists a monotonically decreasing path between some initial set of parameters θ_i and some minimum θ_o identified by some method such as stochastic gradient descent. The insight that this property exists, despite non-convex loss functions and non-linear training sets raises questions, but might be explained by the fact that, given enough data, many problems simply are not that difficult. These results received considerable attention in the field, and the matter is likely to be more complicated. Lucas *et al.*[27] are able to create counterexamples to the MLI property and others have observed different results to Goodfellow *et al.*[26] when revisiting the work on more modern architectures and data sets.[28] Further doubt that 'Machine learning may just be simple' is cast in ref. 29 showing that the MLI does not always hold and must be considered with caution. In general, simply considering a linear interpolation from an initial set of weights to the identified minimum may be insufficient and all the aforementioned papers agree that further study and consideration of the ML-LL is of critical importance. Other work has shown that convergence to a global minimum for overparameterised networks under certain, somewhat restrictive conditions, is provable.[30] These interpretability approaches share the commonality that large areas of the LL and its complex geometric features remain unexplored. In practice is not always guaranteed that the global minimum is identified, and no consideration is given to the shape of the LL

or the existence of other local minima. While such results may be sufficient in terms of performance, it is not helpful in terms of interpretability. Understanding the LL has the potential to provide some of the missing understanding.[31] Specifically, understanding the topography of a loss landscape can allow novel insights into the convergence process or optimiser path taken towards the global minimum.

Another suitable task for global optimisation based LL exploration is the efficient enumeration and analysis of various minima. Using generic tools, surveying large areas of the loss landscape is expensive and time consuming, while the exploration tools outlined below substantially simplify the problem.

Energy landscapes are reasonably well understood for molecules and condensed matter, and the hope exists that some of the associated methodology could help to better understand machine learning. Importantly, since a loss function is ubiquitous in any machine learning system, consideration of the LL is applicable in a broad range of fields. While most work has so far considered neural networks,[20,31] LLs have also been analysed in the context of clustering methods, such as K-means[32] or for Gaussian processes[33] in Bayesian machine learning.[34] These contributions suggest another useful property of the energy landscapes view of machine learning. Entirely different models can now be compared with each other, not just for output metrics such as accuracy, but for the solution landscapes. Understanding how many minima exist for a given model, how they are connected, their relative volumes in parameter space, and how quickly an optimiser converges for them, may provide important insights into model selection.[21]

3 LL exploration

There are a variety of methods developed in chemical physics for exploring potential energy landscapes. Some of these methods are commonly referred to as enhanced sampling, including meta-dynamics,[35] umbrella sampling,[36] and replica-exchange molecular dynamics;[37] a recent review is given by ref. 38. An alternative approach suitable for both potential and loss function surfaces is the energy landscape framework.

Global optimisation algorithms aim to find the lowest minimum, amongst the (possibly) many local minima and funnels. In global optimisation for physical systems popular algorithms are basin-hopping[39–41] and genetic algorithms.[42] In ML, it is common to simply use various random initialisations and local minimisation, which has limited use in physical systems.[43] Examples of random, or pseudo-random, initialisation and minimisation are seen in K-means,[44–46] Gaussian processes,[47] and neural networks. All these methods rely upon minimisation algorithms to locate local minima of the cost function surfaces, and common choices are limited-memory[48,49] quasi-Newton Broyden,[50] Fletcher,[51] Goldfarb,[52] Shanno[53] (L-BFGS) routine and its variants with box-constraints[54,55] for bounded problems such as fitting Gaussian processes. Conjugate gradient approaches can leverage matrix multiplication tricks to address larger datasets,[56,57] and stochastic gradient descent scales well with dataset size due to only considering a portion of the data.[58,59] The choice of minimiser should not change the landscape, but can significantly modify the rate of exploration.

The energy landscape approach is feasible if the number of variables in the fitting space is not too large (up to perhaps 10^4), and the hope is to develop understanding that is transferable to the much larger problems often employed in deep learning models. To analyse the LL using the energy landscape framework, global optimisation is performed initially, the set of low-valued minima are stored, and their connected transition states are located. In a first step, the global minimum of the LL is identified, which is commonly done using basin-hopping global optimisation.[39,40] Starting from any initial values for the parameters, this procedure progresses by local minimisation. Steps to new minima are accepted or rejected, commonly using a Metropolis-type[60] condition, and steps are proposed by perturbing the parameters corresponding to the current minimum in the chain. Local minimisations are usually performed using the LBFGS routine. For a Metropolis accept/reject scheme, a new minimum is always accepted if its energy (loss function) is lower, and is also accepted if the energy is higher with probability

$$P \propto \exp\left(-\frac{\Delta\tilde{E}}{k_{\mathrm{B}}T}\right) \tag{1}$$

where $\Delta\tilde{E}$ is the difference in energy between the new minimum and the old minimum in the chain, k_{B} the Boltzmann constant and T a fictitious temperature. If the energy difference between the old and new minima is large and positive, the move is less likely to be accepted. Uphill steps are needed to escape from traps in the landscape, and the value of the $k_{\mathrm{B}}T$ parameter is chosen to balance local and global exploration.

Local minima do not constitute a landscape. To understand the organisation of solution space, transition states, defined as saddle points with Hessian index one[3] need to be located. Transition states mediate the pathways between minima with the lowest barriers according to the Murrell–Laidler theorem.[3] Here, double-ended searches are usually employed to connect each selected pair of minima, using the doubly-nudged[61,62] elastic band[63–66] method to identify likely candidates for accurate refinement using hybrid-eigenvector following.[67–69] These methods require continuous first and second derivatives, but even for loss functions without these properties, such as K-means, landscapes can still be explored using algorithmic adaptations.[32] These geometry optimisation tools have been refined for a wide range of problems over several decades, and are implemented in the GMIN,[70] OPTIM[71] and PATHSAMPLE[72] programs,[73] all available for use under the GNU General Public License.

Global optimisation and subsequent transition state searches provides the foundations for a full characterisation of the energy landscape/LL of a particular system. This approach is clearly much more computationally expensive than only a single optimisation pass, but the objective here is to understand the structure of the solution space, not to seek predictions for any particular problem. The LL itself is generally unbounded from above. Regularisation methods or other constraints are usually

employed to reduce overfitting problems,[74,75] which tends to keep the fitting parameters within a sensible range.

4 Physical properties and analogues for ML

Machine learning loss landscapes are analogous to energy landscapes and can be interrogated to extract the analogues of thermodynamic and kinetic properties, which constitute the key observables for molecular systems. When characterising a landscape, we can loosely distinguish two sets of metrics: global and local. Global metrics characterise overall properties of the landscape, and local metrics distinguish different types of solutions (*i.e.* minima). The former metrics allow for a characterisation of the whole solution space for archetypal datasets, and provide a better understanding of the nature of the optimisation problem. The distinction is fuzzy and several metrics have important features in both classes. A discussion of some of the most useful properties is given below, and summarised in Table 2.

4.1 Global landscape metrics

4.1.1 Frustration index. The frustration index is a metric that was designed to report on the existence of low-lying minima separated from the global minimum by high barriers.[76] This metric reflects the difficulty of relaxation to the equilibrium occupation probabilities, which will likely correspond to the difficulty of global optimisation on the surface. An important difference between the frustration index, $\mathscr{F}(T)$, and the Shannon entropy,[77] $\mathscr{S}(T)$, is that $\mathscr{F}(T)$ accounts for transition states and barriers, while the Shannon entropy considers only the equilibrium thermodynamic properties of local minima. The Shannon entropy is given by

$$\mathscr{S}(T) = -\sum_{\alpha} p_{\alpha}^{\mathrm{eq}}(T) \ln p_{\alpha}^{\mathrm{eq}}(T), \tag{2}$$

at some temperature, T, and equilibrium occupation probability, p_{α}^{eq}, for minimum α. In contrast, the frustration metric has the form

$$\mathscr{F}(T) = \sum_{\alpha \neq g\,\mathrm{min}} p_{\alpha}^{\mathrm{eq}}(T) \left(\frac{\mathscr{L}_{\alpha}^{\dagger} - \mathscr{L}_{g\,\mathrm{min}}}{\mathscr{L}_{\alpha} - \mathscr{L}_{g\,\mathrm{min}}} \right) \tag{3}$$

where $\mathscr{L}_{\alpha}$ is the loss value of minimum α, and $\mathscr{L}_{\alpha}^{\dagger}$ is the loss value of the highest transition state of the lowest energy path between minimum α and the global minimum. The loss value of the global minimum is denoted $\mathscr{L}_{g\,\mathrm{min}}$. To compare between systems, we can consider $\tilde{\mathscr{F}}(T)$ defined in terms of $\tilde{p}_{\alpha}^{\mathrm{eq}}(T) = p_{\alpha}^{\mathrm{eq}}(T)/(1 - p_{g\mathrm{min}}^{\mathrm{eq}}(T))$. As discussed above, the effective temperature T is simply a parameter to interrogate the landscape in machine learning systems. Studying $\mathscr{S}(T)$ or $\mathscr{F}(T)$ over a range of values for T at the system temperature corresponding to the peaks in heat capacity curves reveals features of the landscape comparable to the analysis of molecular and condensed matter systems in,[76] where various metrics are compared. An example is given in Fig. 2. Here, the landscape on the left is an ideal single funnel, where locating the global minimum is straightforward over a wide range of temperatures. In contrast, locating the true global minimum for the landscape on the right is more difficult. However, if alternative low-lying minima provide good solutions then it will be straightforward to locate a member of this set. Importantly, the alternative minima will probably have different properties, and perhaps provide slightly different predictions. Nevertheless, this structure may be more robust to initialisation noise and multiple such minima could be combined in ensembles to improve overall accuracy. In machine learning applications, $\tilde{\mathscr{F}}(T)$ has important effects on training reproducibility and may correlate with batching effects. Since the same minimum is more likely to be found repeatedly in unfrustrated landscapes, training these systems is more reproducible and variation in output is less likely to come from initialisation noise. High-frustration surfaces may further be more prone to batch effects, or at least have increased variance with batch effects. Like above, this is due to the high likelihood of individual minima being overfit to specific aspects of the input data.

4.1.2 Heat capacity. The heat capacity of a system is defined as the amount of energy (heat) that has to be added to achieve a unit change in temperature. Wales[78] describes a theoretical framework that enables features of the heat capacity to be connected to particular local minima in the energy landscape. Normal mode analysis for each minimum allows a harmonic superposition approximation to the vibrational density of states. Given the partition function for some minimum α

$$Z_{\alpha}(T) = \frac{2\prod_{s} N_s!}{o_{\alpha}} \left(\frac{k_{\mathrm{B}}T}{h\bar{\nu}_{\alpha}} \right)^{\kappa} \mathrm{e}^{-V_{\alpha}/k_{\mathrm{B}}T} \equiv n_{\alpha} \left(\frac{k_{\mathrm{B}}T}{h\bar{\nu}_{\alpha}} \right)^{\kappa} \mathrm{e}^{-V_{\alpha}/k_{\mathrm{B}}T}, \tag{4}$$

where $\kappa = 3N - 6$ is the number of vibrational degrees of freedom for N atoms, k_{B} the Boltzmann constant, $\bar{\nu}_{\alpha}$ the geometric mean normal mode vibrational frequency, a measure of basin geometry, o_{α} the order of the molecular point group, T the temperature and V_{γ} the potential energy of minimum γ, the corresponding internal energy E and heat capacity C_{V} can be derived. By defining the harmonic superposition partition

Table 2 Interpretation of physical characteristics for molecular energy landscapes and machine learning LLs

Feature	Molecular PES	ML LL
Basin volume	Entropic contribution to occupation probability	Connection to robustness
Heat capacity	Change in occupied minima as a function of temperature	Identification of minima with complementary properties
Frustration	Propensity for broken ergodicity	Implications for optimisation and training

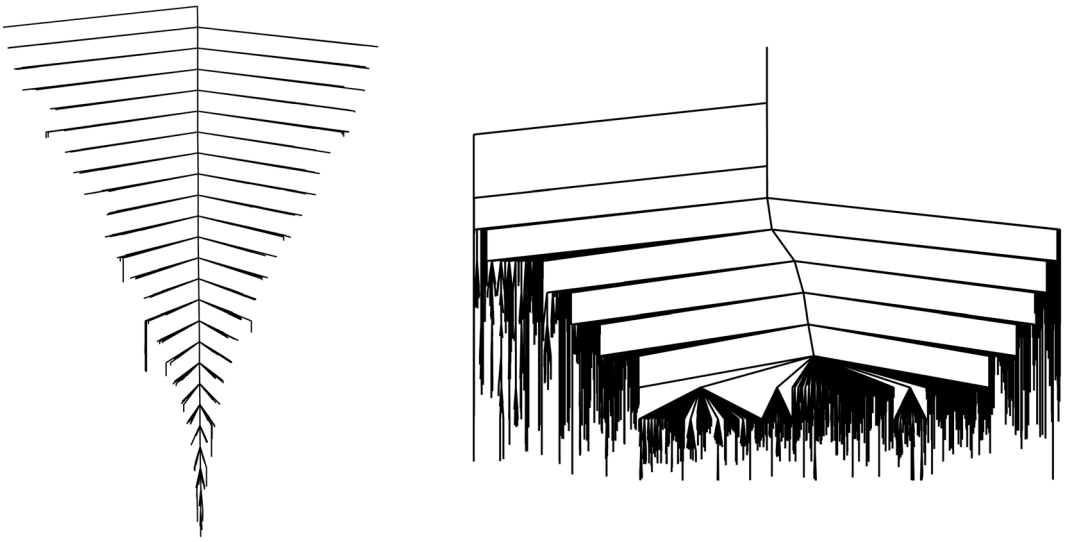

Fig. 2 Examples for two distinct loss landscapes, visualised using disconnectivity graphs, with drastically different frustration indices. The landscape on the left is an ideal single funnel, while the landscape on the right has many low-lying minima (acceptable solutions), which are equally accessible, potentially making this landscape more robust.

function, and using some elementary identities, a novel formulation of the heat capacity can be derived.[78] Peaks in the heat capacity curve can be interpreted by looking at the contribution of minima with positive and negative temperature derivatives

$$C_V = \kappa k_B + \sum_{\gamma}^{g_\gamma(T)>0} g_\gamma(T)\left(V_\gamma - \langle V\rangle_{\min}\right) + \sum_{\gamma}^{g_\gamma(T)<0} g_\gamma(T)\left(V_\gamma - \langle V\rangle_{\min}\right)$$
$$\equiv \kappa k_B + C^+(T) + C^-(T) \quad (5)$$

This analysis tells us how the occupation probability shifts between local minima as a function of the temperature parameter. Around specific peaks in the heat capacity, some minima contribute positively (increased occupation probability), while others contribute negatively (lowered occupation probability). This effect is visualised in Fig. 3, where the positively and negatively contributing minima for two peaks in the heat capacity curve are visualised. Note that substantially more minima contribute around the larger peak in the C_V curve.

In molecular systems, peaks in the heat capacity correspond to solid–solid or solid–liquid phase transitions, where the system moves between qualitatively different sets of local minima, associated with different energy and entropy. For ML systems, the analogue of the heat capacity reveals how the occupation of minima changes with the temperature parameter. The temperature in an ML problem is fictitious (Fig. 3), but serves as a parameter to scan the properties of the landscape and report on changes that highlight qualitatively different solutions (local minima). Minima separated by a high energy barrier may be very different,[79] although degenerate solutions can also exist due to symmetries of the loss function.[80] In fact, it has been shown in one example that different minima may 'specialise' in different parts of the input data, so that better predictions can be obtained by employing alternative solutions from the LL for different input. The heat capacity provides a way to identify these 'different' minima with contrasting properties. In applications such as ensemble learning, this capability is highly relevant. Combining different minima enhances ensemble methods significantly beyond randomly choosing a subset of minima.[80]

4.1.3 Network properties. The representation of the continuous surface by a weighted graph, or kinetic transition network[81–84] allows graph algorithms to be applied to generate physical insight. One useful class of algorithms address community detection, and when applied to kinetic transition networks generate a set of solutions that are dynamically distinct.[85,86] Members of the same community interconvert on a timescale much shorter than those in different communities. Understanding the partitioning of solutions based not on Euclidean distance, but the topography, gives a more accurate picture of the time evolution of a physical system, and the distinctness of different solutions. The ability to move beyond Euclidean distance in evaluating the distinctness of models may be promising for developing ensemble models that capture all the relevant information.

Furthermore, the degree of each minimum, *i.e.* the number of direct connections to other minima *via* a single transition state, is a useful property. Nodes with a high degree constitute hubs, associated with small world properties. These minima are usually easy to locate during optimisation, and they are key to moving between different regions of the space. For physical systems it tends to be low-valued solutions that act as hubs, which can explain whether they are easy to locate.[87,88] The degree of a node can also highlight its importance to

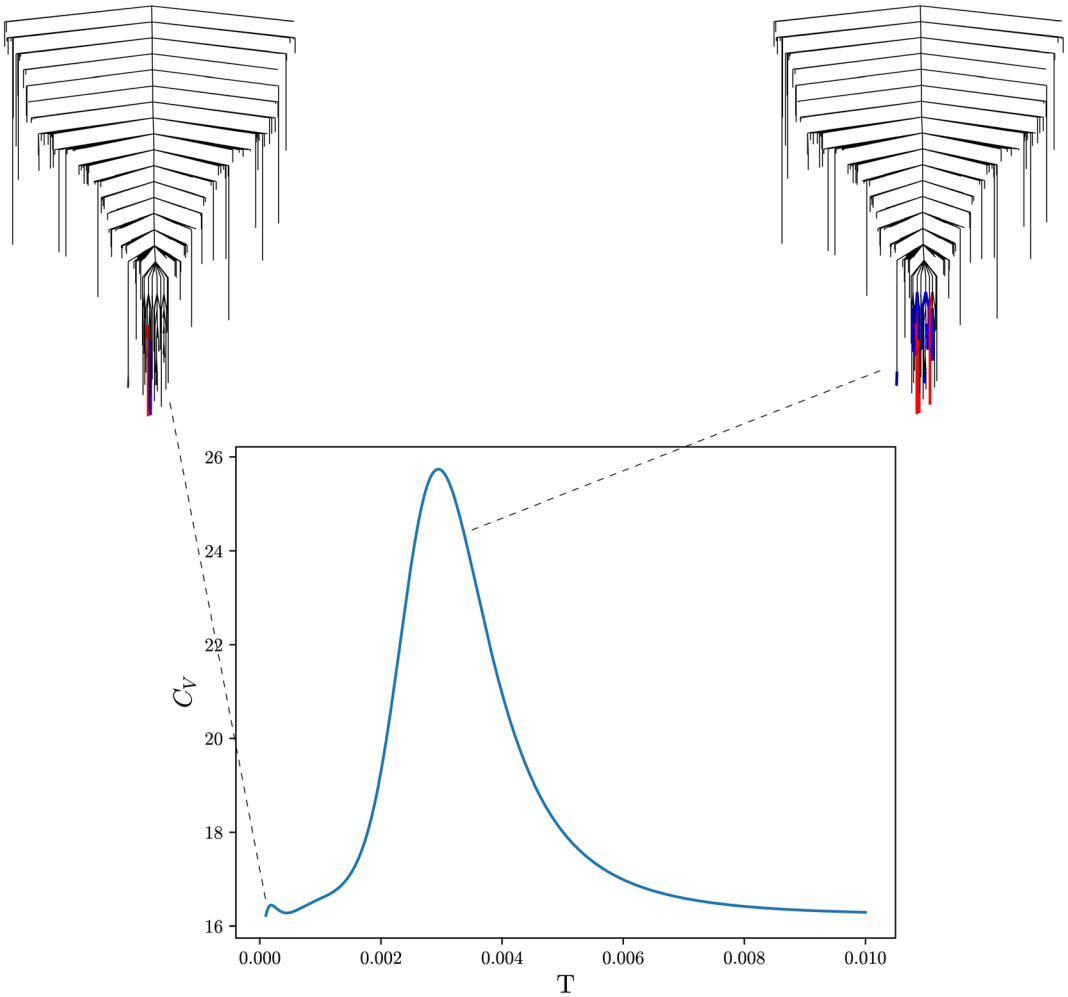

Fig. 3 Heat capacity curve for a machine learning loss landscape. The loss landscape is visualised using disconnectivity graphs. Both graphs show the same landscape, highlighted are the positive and negative contributions to the heat capacity curve for the smaller (left) and larger (right) peak in blue and red respectively.

optimisation algorithms in physical systems and abstract cost functions. Furthermore, the distribution of node degrees, which is a global property of the system, can be used to understand the organisation of the landscape.[89]

4.2 Local landscape metrics

4.2.1 Rates. Rates are an essential quantity in computing the time-evolution of physical systems. The rate constant between two minima that are directly connected by a transition state is computed using unimolecular rate theory.[90,91] From these elementary steps one can build a global view of dynamics by combining them. Rates between sets of minima are calculated for a complete network using the graph transformation algorithm.[92,93] Rates have been used to analyse time evolution of many solid-state[94] and biomolecular[95,96] systems, and rate calculations have been extended to *K*-means clustering.[32] A recent review of numerical rate calculations is given in ref. 97

In ML systems, rates have no physical analogue, but they nevertheless provide a useful estimate of the difficulty in moving between different regions of solution space. The rates, calculated with the contributions of all known solutions, account for both intervening barriers in the loss function and the number of intermediate minima. Both properties have physical meaning for understanding the solution space, and contain important additional information not present in distance calculations. Small rates indicate that two given minima are highly distinct, where interconversion requires either many, or large, changes in model parameters.

4.2.2 Monotonic sequence basins. Monotonic sequence basins (MSBs) are minima not directly connected to any lower-valued minima. Reducing a landscape to its monotonic sequence basins allows a significant reduction in complexity. In complex systems, hundreds of minima may be well represented by only a handful of states. This representation contains all optimal solutions within their surrounding regions of space. Furthermore, the number of MSBs can be seen as a proxy for the number of funnels, which are distinct regions of the landscape associated with different molecular configurations or weights/hyperparameters.

4.2.3 Catchment basin volume. The basin of attraction,[1,98] for any given minimum, is the set of points for which steepest-decent paths converge to that structure. This region has a well-defined volume in configuration space. A Taylor expansion to second order in the vicinity of a local minimum enables the corresponding partition function to be computed in terms of the log product of positive Hessian eigenvalues (LPPHE) for the Hessian matrix of second derivatives. The corresponding configuration volume (or density of states) is related to the harmonic vibrational entropy in an atomic system, and the log product of positive eigenvalues is a convenient measure of the 'width' associated with a local minimum for a loss landscape. The occupation probability for a given minimum as a function of the temperature parameter depends on the balance between the energy (loss function), which appears as a Boltzmann factor, and the entropy, which is determined by the (generally anharmonic) density of states in the catchment basin. The rate at which this equilibrium value is achieved, if we define the analogue of chemical kinetics, depends on the barriers between minima and the global organisation of the landscape.

Accurate values for the analogue properties of LL minima are not required to diagnose the existence of qualitatively different solutions, and hence the harmonic value reported by the LPPHE is sufficient for diagnostic purposes. The configuration volume for a basin of attraction may also have useful interpretations in ML problems. One of the most important features of a machine learning model is that is should be robust. The LPPHE provides a harmonic measure of the basin volume[31] which allows minima to be selected based on some intuition of how robust they might be, as well as training accuracy. We emphasise once again, that the value of the effective heat capacity is not important here, but peaks in this function enable us to identify local minima with distinct classification properties in an efficient manner.

4.3 Further possibilities

The machine learning community has only recently begun to explore the analogues of physically observable thermodynamic and kinetic properties for machine learning loss landscapes. In particular, little work has been done to determine whether dynamical analogues might be useful. As for thermodynamic quantities, such as the heat capacity, there could be useful insight to be gained from understanding how such quantities report on the nature of the machine learning solution space.

4.4 ML model metrics

Above, we have discussed various metrics that are relevant when considering the energy landscape of an atomistic system, and how these may be applied to ML systems. We now want to briefly discuss metrics that are considered in machine learning, implicitly characterising ML LLs. As described above, the LL is at best a surrogate of quality: since it is only based on training data, the ability to generalise to testing data is not easily obtainable. The same imperfect correlation between loss function and quality is seen in unsupervised clustering methods, such as *K*-means, even without the presence of test data.

In practice, ML models are largely scored for accuracy and robustness, *i.e.* test accuracy. A practitioner may be interested in how the loss value changes on training data, and perhaps also in training loss. Yet, results are usually reported on test datasets. A helpful review of machine learning evaluation can be found in ref. 99. In general, the relevant metrics in machine learning models are largely results-focused and only to a lesser degree incorporate an understanding of the system. As long as the test accuracy in terms of MSE, AUC, or top-k loss is sufficient, the practitioner rarely cares about interpretation in terms of the Hessian eigenvalues of the underlying loss landscape. Such physical quantities have a clear meaning in energy landscapes, and they are routinely analysed. We hope that by translating some of these metrics into practical machine learning understanding, more attention will be paid to these metrics in the future.

5 Applications of EL4ML

Here we will discuss applications where knowledge of the LL has been used to understand or improve machine learning. Fig. 4 provides an overview of the four application areas we consider as most promising for loss landscape methods.

5.1 Robustness

Incorporating knowledge of the loss landscape has become increasingly common in machine learning. Most prominently, several new optimisation methods have been developed that include some degree of information about the gradient of the LL.[100–103] Including information about the LL in optimisation seems to lead to improved robustness of the solution. Robustness in machine learning refers to the ability of a particular model to generalise well to unseen testing data. A more robust model will perform better on testing data than a model that is overfit on the training data and does not generalise well. Flatter minima, geometrically characterised by Hessian eigenvalues (curvatures) with smaller magnitudes, are expected to be more robust.[104–106] This result seems intuitive, since it means that if slightly different training data displace the minimum from its given position, it will still be close to the original position for a 'flatter' landscape, whereas the resulting displacement may be larger when the local curvatures are greater.

Mathematically, given a minimum at position $\mathbf{P}$ with energy/loss $\mathscr{E}$, a small displacement of $\mathbf{P}+\mathbf{p}$, caused by slightly different training data, will have an effect on $\mathscr{E}$ depending on the curvatures around $\mathbf{P}$, *i.e.* $\Delta\mathscr{E} = \frac{1}{2}\mathbf{p}^{\mathrm{T}}\mathbf{H}(\mathbf{P})\mathbf{p}$, where $\mathbf{H}(\mathbf{P})$ is the Hessian at $\mathbf{P}$. Hence, if the Hessian, and more specifically its eigenvalues, are larger, the minimum is 'narrower' and the difference in $\mathscr{E}$, $\Delta\mathscr{E}$ between positions $\mathbf{P}$ and $\mathbf{P}+\mathbf{p}$ is greater, the minimum is less robust. Foret *et al.*[101] have included knowledge about the shape of the loss function and managed to find more robust minima. Overall, robustness is one of the most important concepts in machine learning.[107] A completely overfit model, one that has perfect training accuracy, but does not generalise at all to testing data, is useless in practice. Thus,

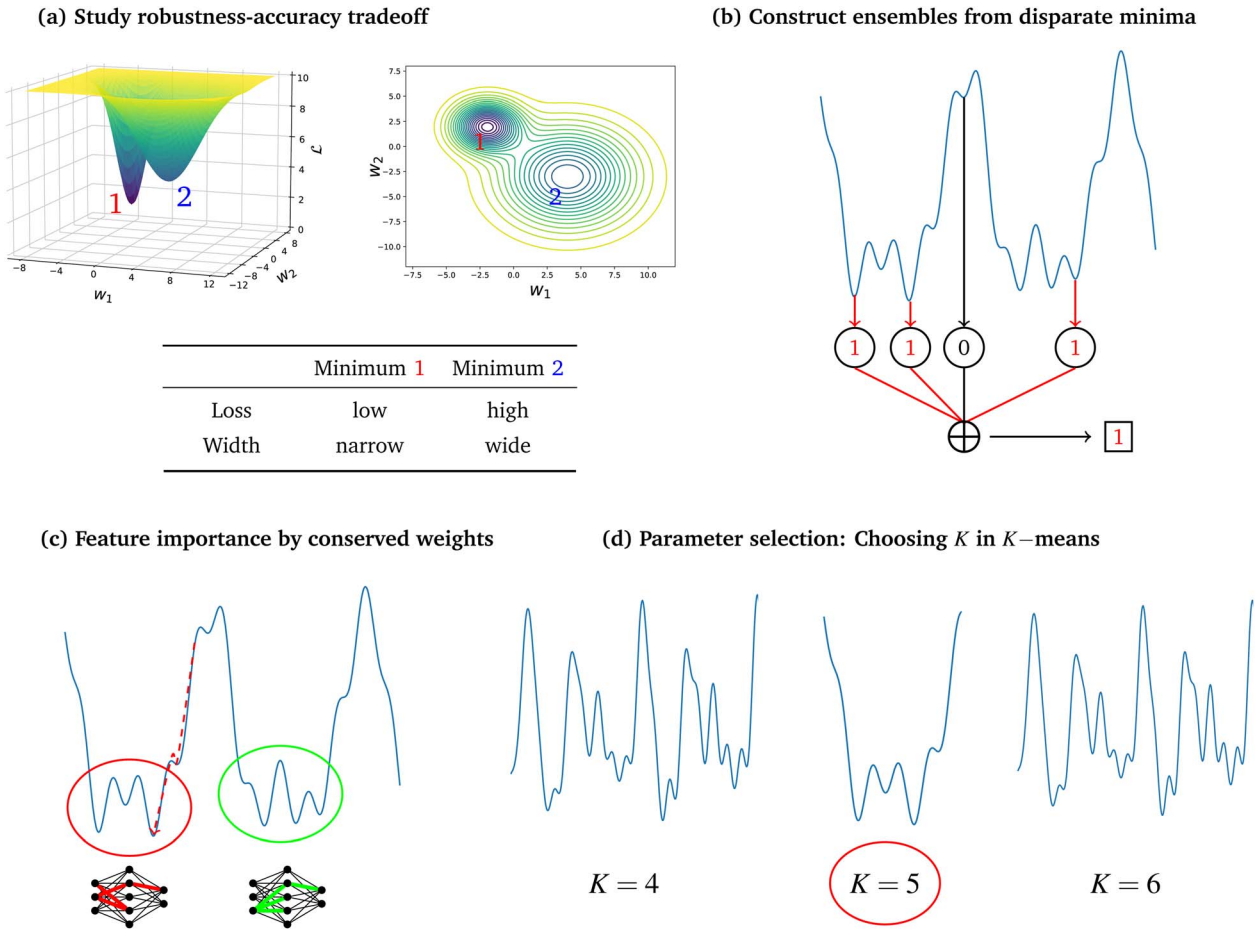

	Minimum 1	Minimum 2
Loss	low	high
Width	narrow	wide

Fig. 4 Four applications areas of energy landscapes methods in machine learning with specific examples. (a) Robustness: insights into the relative curvature around minima can be generated from a landscapes perspective, providing a quantification of model robustness. (b) Ensembles: qualitatively different minima can be identified from the loss landscape and selected for ensemble models. (c) Interpretability: identify weights conserved across minima and visualise model training descent path. (d) Parameter selection: landscape geometry and number of funnels can be used as a method for parameter selection in algorithms such as K-means.

considering geometric features of the loss landscape may be an important way in combating this problem.

5.2 Ensemble methods

Knowledge of the loss landscape may help improve prediction accuracy for a given model. Ensemble methods, combining or averaging multiple predictors for a single task, is a well established approach.[108–111] One reason why ensemble methods have become so important over previous years is the imperfect correlation of performance and loss resulting from limited training data. The single best minimum is often not sufficient and hence, a combination of so called weak learners is required to outperform a 'better' minimum. Related challenges arise in batch selection for Bayesian optimisation, where the key challenge is determining a diverse set of samples for the task of maximising an expensive 'black-box' function.[112–116] Two of the critical design choices in ensemble learning are, which classifiers to combine, and how to combine them. Common approaches include bagging and boosting methods, which are well described in ref. 117. The possible approaches to combine predictions of different minima range from simple majority votes, to complex weighting schemes for the contribution of individual classifiers. The same methods can be applied to unsupervised learning, where clustering solutions can be combined to improve separation, without the separation into training and testing data.[118] The value of ensemble learning arises when different classifiers are good at classifying different subsets of the data, or prioritise different parts of the input. Recently, the idea of combining multiple minima of the LL, obtained *via* energy landscapes methodology,[80] has been examined. Each minimum can be viewed as an individual classifier, where all models have the same architecture, but very different parameters. Combining classifiers, all obtained from one LL, provides the distinct advantage that the classifiers are known to be qualitatively 'different', which is the key feature in ensemble learning. Specifically, for some LL, standard measures based on analogue properties from the physical sciences, such as the heat capacity, can be analysed to increase the likelihood that the minima are complementary. Landscape guided ensemble learning is another example of how physics-inspired machine learning can outperform common methods, and hence provide significant additional performance.

5.3 Interpretability

Understanding the black box of machine learning systems is one of the greatest challenges to the field today. Various gradient and perturbation based methods exist,[119] yet their usefulness and accuracy is debated, and is not generally agreed to be sufficient.[120] Hence, alternative ways to improve our understanding of decision-making by a particular model are desirable. Studying individual funnels of the landscape, as seen in disconnectivity graphs, may provide a promising way to increase interpretability. This approach is commonly exploited in the molecular sciences[121,122] where a multifunnelled landscape is analysed to understand which structural differences of a molecule constitute a group of solutions in a specific funnel. The machine learning analogue is that for a multi-funnelled landscape, one can compute the sets of parameters that characterise a particular funnel, as in ref. 123. These parameters, conserved across multiple minima, are therefore likely to be important in the model, and may guide interpretability.

5.4 Selecting overall parameters

ML algorithms can involve choosing a parameter that is not itself part of the optimisation problem. A prominent example is the choice of cluster number, K, in K-means. Each K defines a distinct cost function surface that must be optimised to generate low-valued clustering solutions. The choice of the appropriate cluster number is usually made using one, or a small set, of solutions at each K,[124–127] reviewed in ref. 128. However, it is possible to make this decision using the topography of the whole solution space, rather than a small number of solutions. The use of landscapes, composed of many solutions, increases the reproducibility, as there is less dependence on locating certain minima, amongst a vast number, when computing metrics. The presence of certain landscape structure is indicative of an appropriate number of clusters, as observed for clustering gene expression data to identify cancer subtypes.[129] Such an analysis is significantly more expensive than characterising single minima, but for many applications, the quality and reproducibility of the solution are essential.

6 Future work

Many applications of energy landscapes remain unexplored in the context of machine learning. In this section, we will outline a few interesting areas of future work that would build substantially on the energy landscapes methodology. Firstly, it will be interesting to see advances in understanding the physics-inspired analogues of machine learning. For example, understanding in more detail the relationship between minima contributing to the heat capacity and the importance (both in terms of accuracy and robustness) of these minima in an inference task. Furthermore, many other concepts, such as the dynamical analogues in machine learning systems, remain largely unexplored. Understanding the usefulness of such metrics may give further insights from the physical sciences to the more abstract, black-box world of machine learning. In general, physics-inspired machine learning seems to be a good candidate for improving our understanding of machine learning, by transferring knowledge from a relatively mature field, to a newer one.

Another area in which the energy landscape approach may prove very helpful is Bayesian inference using Gaussian processes (GPs). An inherent challenge within these methods is identifying suitable hyperparameters. Most commonly, a loss function, usually the log marginal likelihood, is maximised and a single point estimate is taken for the hyperparameters. However, single-point estimates may be insufficient when there are multiple competing fits.[130] A common method to overcome the limitations of single point estimates is Monte Carlo (MC) sampling of the hyperparameter distribution.[131–133] Previous work has used sequential MC sampling,[130,134] Bayesian MC sampling,[135] and Hamiltonian MC sampling.[136] Additionally, slice sampling,[137] adaptive importance sampling,[138] and entropy-based methods[139] have been used within Bayesian optimisation, where there is interest in moving beyond single-point estimates to fully-Bayesian approaches.[140,141] The main drawback with these methods is the high computational cost, and ideally they should only be employed when it will provide a substantial advantage over single point estimates. However, this condition cannot be known *a priori*. Looking at the loss landscape may provide an answer. There may be a direct relationship between the number of funnels in the landscape, perhaps characterised by monotonic sequence basins, or the frustration index, and the effect that MC sampling has on improving accuracy and generalisability over single point estimates. Thus, knowledge of the landscape, obtained *via* appropriate sampling, could lead to a substantial reduction in compute cost by identifying when a fully-Bayesian approach is required. Moreover, the additional information present in landscapes may extend existing variational inference methods[142,143] by allowing more accurate approximate distributions to be generated and sampled.

7 Conclusions

Important relationships exist between physical molecular energy landscapes and abstract machine learning loss landscapes. In this contribution we have highlighted some of the recent work on physics-inspired machine learning and how theoretical methods from one field may be applied to the other. We have discussed how various metrics, such as the heat capacity, catchment basin volume, or frustration index can help to improve and explain robustness, accuracy, and importantly interpretability in machine learning. Many of the connections between these two fields remain to be explored and exploited.

Energy landscapes provide important insight to answer questions in machine learning, irrespective of the underlying model, because they focus on the structure of the solution space. More generally, exploiting a well understood methodology is a promising approach to vastly increase the set of problems that machine learning can be applied to. The hope is that methods from the physical sciences can work in conjunction with machine learning methods to give practitioners more trust and confidence in their predictions, as well as greater

understanding of what a given model is actually doing. Ultimately, this approach could facilitate further growth in the influence that machine learning has on society as a whole.

Data availability

In this review article, no novel data was analysed or studied.

Conflicts of interest

There are no conflicts to declare.

Acknowledgements

DJW gratefully acknowledges an International Chair at the Interdisciplinary Institute for Artificial Intelligence at 3iA Cote d'Azur, supported by the French government, with reference number ANR-19-P3IA-0002, which has provided interactions that furthered the present research project. MPN acknowledges funding from Downing College, Cambridge. LD and EOP-K would like to acknowledge this work was supported by the Hartree National Centre for Digital Innovation – a collaboration between Science and Technology Facilities Council and IBM. LD also acknowledges the financial support of the EPSRC *via* a knowledge transfer fellowship.

Notes and references

1 D. J. Wales, *Energy Landscapes*, Cambridge University Press, Cambridge, 2003.
2 J. A. Joseph, K. Röder, D. Chakraborty, R. G. Mantell and D. J. Wales, *Chem. Commun.*, 2017, **53**, 6974–6988.
3 J. N. Murrell and K. J. Laidler, *Trans. Faraday Soc.*, 1968, **64**, 371–377.
4 D. Silver, T. Hubert, J. Schrittwieser, I. Antonoglou, M. Lai, A. Guez, M. Lanctot, L. Sifre, D. Kumaran, T. Graepel *et al.*, *arXiv*, 2017, preprint arXiv:1712.01815, DOI: **10.48550/arXiv.1712.01815**.
5 D. Silver, J. Schrittwieser, K. Simonyan, I. Antonoglou, A. Huang, A. Guez, T. Hubert, L. Baker, M. Lai, A. Bolton, *et al.*, *Nature*, 2017, **550**, 354–359.
6 C. Berner, G. Brockman, B. Chan, V. Cheung, P. Debiak, C. Dennison, D. Farhi, Q. Fischer, A. Hashme, C. Hesse *et al.*, *arXiv*, 2019, preprint arXiv:1912.06680, DOI: **10.48550/arXiv.1912.06680**.
7 S. Grigorescu, B. Trasnea, T. Cocias and G. Macesanu, *J. Field Robot.*, 2020, **37**, 362–386.
8 J. Jumper, R. Evans, A. Pritzel, T. Green, M. Figurnov, O. Ronneberger, K. Tunyasuvunakool, R. Bates, A. Žídek, A. Potapenko, *et al.*, *Nature*, 2021, **596**, 583–589.
9 A. Davies, P. Veličković, L. Buesing, S. Blackwell, D. Zheng, N. Tomašev, R. Tanburn, P. Battaglia, C. Blundell, A. Juhász, *et al.*, *Nature*, 2021, **600**, 70–74.
10 P. Budzianowski and I. Vulić, *arXiv*, 2019, preprint arXiv:1907.05774, DOI: **10.48550/arXiv.1907.05774**.
11 T. Brown, B. Mann, N. Ryder, M. Subbiah, J. D. Kaplan, P. Dhariwal, A. Neelakantan, P. Shyam, G. Sastry, A. Askell *et al.*, *Advances in neural information processing systems*, 2020, vol. 33, pp. 1877–1901.
12 A. Ramesh, P. Dhariwal, A. Nichol, C. Chu and M. Chen, *arXiv*, 2022, preprint, arXiv:2204.06125. DOI: **10.48550/arXiv.2204.06125**.
13 R. Gal, Y. Alaluf, Y. Atzmon, O. Patashnik, A. H. Bermano, G. Chechik and D. Cohen-Or, *arXiv*, 2022, preprint, arXiv:2208.01618, DOI: **10.48550/arXiv.2208.01618**.
14 F. Noé, A. Tkatchenko, K. Müller and C. Clementi, *Annu. Rev. Phys. Chem.*, 2020, **71**, 361–390.
15 Y. Cooper, *arXiv*, 2018, preprint, arXiv:1804.10200, DOI: **10.48550/arXiv.1804.10200**.
16 Y. Zhang, P. Tiňo, A. Leonardis and K. Tang, *IEEE Transactions on Emerging Topics in Computational Intelligence*, 2021.
17 Q. Zhang and S. Zhu, *Front. Inf. Technol. Electron. Eng.*, 2018, **19**, 27–39.
18 L. H. Gilpin, D. Bau, B. Z. Yuan, A. Bajwa, M. Specter and L. Kagal, *2018 IEEE 5th International Conference on data science and advanced analytics*, DSAA, 2018, pp. 80–89.
19 Z. C. Lipton, *Queue*, 2018, **16**, 31–57.
20 A. J. Ballard, R. Das, S. Martiniani, D. Mehta, L. Sagun, J. D. Stevenson and D. J. Wales, *Phys. Chem. Chem. Phys.*, 2017, **19**, 12585–12603.
21 M. P. Niroomand, C. T. Cafolla, J. W. R. Morgan and D. J. Wales, *Mach. Learn.: Sci. Technol.*, 2022, **3**, 015019.
22 S. R. Chitturi, P. C. Verpoort, D. J. Wales, *et al.*, *Mach. Learn.: Sci. Technol.*, 2020, **1**, 023002.
23 M. V. Narkhede, P. P. Bartakke and M. S. Sutaone, *Artif. Intell. Rev.*, 2022, **55**, 291–322.
24 F. Draxler, K. Veschgini, M. Salmhofer and F. Hamprecht, *International conference on machine learning*, 2018, pp. 1309–1318.
25 B. Neyshabur, S. Bhojanapalli, D. McAllester and N. Srebro, *Advances in neural information processing systems*, 2017, vol. 30.
26 I. J. Goodfellow, O. Vinyals and A. M. Saxe, *arXiv*, 2014, preprint, arXiv:1412.6544, DOI: **10.48550/arXiv.1412.6544**.
27 J. Lucas, J. Bae, M. R. Zhang, S. Fort, R. Zemel and R. Grosse, *arXiv*, 2021, preprint, arXiv:2104.11044, DOI: **10.48550/arXiv.2104.11044**.
28 J. Frankle, *arXiv*, 2020, preprint, arXiv:2012.06898, DOI: **10.48550/arXiv.2012.06898**.
29 T. J. Vlaar and J. Frankle, *International Conference on Machine Learning*, 2022, pp. 22325–22341.
30 S. Du, J. Lee, H. Li, L. Wang and X. Zhai, *International conference on machine learning*, 2019, pp. 1675–1685.
31 P. C. Verpoort, A. A. Lee and D. J. Wales, *Proc. Natl. Acad. Sci. U. S. A.*, 2020, **117**, 21857–21864.
32 L. Dicks and D. J. Wales, *J. Chem. Phys.*, 2022, **156**, 054109.
33 M. Chouza, S. Roberts and S. Zohren, *arXiv*, 2018, preprint, arXiv:1803.09119, DOI: **10.48550/arXiv.1803.09119**.
34 C. E. Rasmussen, *Summer school on machine learning*, 2003, pp. 63–71.
35 A. Laio and M. Parrinello, *Proc. Natl. Acad. Sci. U. S. A.*, 2002, **99**, 12562–12576.

36 G. M. Torrie and J. P. Valleau, *Chem. Phys. Lett.*, 1974, **28**, 578.
37 Y. Sugita and Y. Okamoto, *Chem. Phys. Lett.*, 1999, **314**, 141.
38 J. Hénin, T. Leliévre, M. R. Shirts, O. Valsson and L. Delemotte, *Living J. Comput. Mol. Sci.*, 2022, **4**, 1583.
39 Z. Li and H. A. Scheraga, *Proc. Natl. Acad. Sci. U. S. A.*, 1987, **84**, 6611–6615.
40 D. J. Wales and J. P. K. Doye, *J. Phys. Chem. A*, 1997, **101**, 5111.
41 D. J. Wales and H. A. Scheraga, *Science*, 1999, **285**, 1368–1372.
42 E. S. Henault, M. H. Rasmussen and J. H. Jensen, *ChemRxiv*, 2020, DOI: **10.26434/chemrxiv.12152661.v1**.
43 C. J. Pickard and R. J. Needs, *J. Phys.: Condens.Matter*, 2011, **23**, 053201.
44 D. Arthur and S. Vassilvitskii, *Proc. of the 18th Ann. ACM-SIAM Symp. on Discrete Algorithms*, 2007, pp. 1027–1035.
45 A. H. Mohammad, C. Vineed, S. Saeed and J. Z. Mohammed, *Pattern Recognit. Lett.*, 2009, **30**, 994–1002.
46 O. Bachem, M. Lucic, S. H. Hassani and A. Krause, *Proc. of the 30th Int. Conf. on Neural Information Processing Systems*, 2016, pp. 55–63.
47 C. E. Rasmussen and C. K. I. Williams, *Gaussian processes for machine learning*, MIT Press, 2005.
48 D. C. Liu and J. Nocedal, *Math. Program.*, 1989, **45**, 503–528.
49 J. Nocedal, *Math. Comput.*, 1980, **35**, 773–782.
50 C. G. Broyden, *J. Inst. Math. Its Appl.*, 1970, **6**, 76–90.
51 R. Fletcher, *Comput. J.*, 1970, **13**, 317–322.
52 D. Goldfarb, *Math. Comput.*, 1970, **24**, 23–26.
53 D. F. Shanno, *Math. Comput.*, 1970, **24**, 647–656.
54 R. H. Byrd, P. Lu, J. Nocedal and C. Zhu, *SIAM J. Sci. Comput.*, 1995, **16**, 1190–1208.
55 C. Zhu, R. H. Byrd, P. Lu and J. Nocedal, *ACM Trans. Math. Softw.*, 1997, **23**, 550–560.
56 K. A. Wang, G. Pleiss, J. R. Gardner, S. Tyree, K. Q. Weinberger and A. G. Wilson, *NeurIPS*, 2019.
57 J. Wenger, G. Pleiss, P. Hennig, J. Cunningham and J. Gardner, *Proc. Mach. Learn. Res.*, 2022, **162**, 23751–23780.
58 D. P. Kingma and J. L. Ba, 2015, preprint, arxiv:1412.6980, DOI: **10.48550/arXiv.1412.6980**.
59 L. Bottou, F. E. Curtis and J. Nocedal, *SIAM Rev.*, 2018, **60**, 1.
60 N. Metropolis, A. W. Rosenbluth, M. N. Rosenbluth, A. H. Teller and E. Teller, *J. Chem. Phys.*, 1953, **21**, 1087–1092.
61 S. A. Trygubenko and D. J. Wales, *J. Chem. Phys.*, 2004, **120**, 2082–2094.
62 D. Sheppard, R. Terrell and G. Henkelman, *J. Chem. Phys.*, 2008, **128**, 134106.
63 G. Mills, H. Jónsson and G. K. Schenter, *Surf. Sci.*, 1995, **324**, 305–337.
64 H. Jónsson, G. Mills and K. W. Jacobsen, *Classical and quantum dynamics in condensed phase simulations*, World Scientific, Singapore, 1998, ch. 16, pp. 385–404.
65 G. Henkelman, B. P. Uberuaga and H. Jónsson, *J. Chem. Phys.*, 2000, **113**, 9901–9904.
66 G. Henkelman and H. Jónsson, *J. Chem. Phys.*, 2000, **113**, 9978–9985.
67 L. J. Munro and D. J. Wales, *Phys. Rev. B: Condens. Matter Mater. Phys.*, 1999, **59**, 3969–3980.
68 G. Henkelman and H. Jónsson, *J. Chem. Phys.*, 1999, **111**, 7010–7022.
69 Y. Kumeda, L. J. Munro and D. J. Wales, *Chem. Phys. Lett.*, 2001, **341**, 185–194.
70 *GMIN: A program for basin-hopping global optimisation, basin-sampling, and parallel tempering*, **http://www-wales.ch.cam.ac.uk/software.html**.
71 *OPTIM: A program for geometry optimisation and pathway calculations*, **http://www-wales.ch.cam.ac.uk/software.html**.
72 *PATHSAMPLE: A program for generating connected stationary point databases and extracting global kinetics*, **http://www-wales.ch.cam.ac.uk/software.html**.
73 *pylfl: A Python package to survey LFLs in ML models*.
74 G. C. Cawley and N. L. C. Talbot, *J. Mach. Learn. Res.*, 2007, **8**, 841–861.
75 J. Chen, K. de Hoogh, J. Gulliver, B. Hoffmann, O. Hertel, M. Ketzel, M. Bauwelinck, A. Van Donkelaar, U. A. Hvidtfeldt, K. Katsouyanni, *et al.*, *Environ. Int.*, 2019, **130**, 104934.
76 V. K. De Souza, J. D. Stevenson, S. P. Niblett, J. D. Farrell and D. J. Wales, *J. Chem. Phys.*, 2017, **146**, 124103.
77 C. E. Shannon, *Bell Syst. Tech. J.*, 1948, **27**, 379–423.
78 D. J. Wales, *Phys. Rev. E*, 2017, **95**, 030105.
79 A. V. Bradley, C. A. Gomez-Uribe and M. R. Vuyyuru, *Mach. Learn.: Sci. Technol.*, 2022, **3**, 045002.
80 M. P. Niroomand, J. W. R. Morgan, C. T. Cafolla and D. J. Wales, *Mach. Learn.: Sci. Technol.*, 2022, **3**, 025004.
81 D. J. Wales, *Int. Rev. Phys. Chem.*, 2006, **25**, 237–282.
82 F. Noé and S. Fischer, *Curr. Opin. Struct. Biol.*, 2008, **18**, 154–162.
83 J. M. Carr and D. J. Wales, *Phys. Chem. Chem. Phys.*, 2009, **11**, 3341–3354.
84 D. Prada-Gracia, J. Gómez-Gardenes, P. Echenique and F. Falo, *PLoS Comput. Biol.*, 2009, **5**, e1000415.
85 C. P. Massen and J. P. K. Doye, *Phys. Rev. E*, 2005, **71**, 046101.
86 D. Kannan, D. J. Sharpe, T. D. Swinburne and D. J. Wales, *J. Chem. Phys.*, 2020, **153**, 244108.
87 J. P. Doye and C. P. Massen, *J. Chem. Phys.*, 2005, **122**, 084105.
88 J. P. K. Doye and C. P. Massen, *arXiv*, 2007, preprint, arxiv:cond-mat/0612150, DOI: **10.48550/arXiv.cond-mat/0612150**.
89 J. W. R. Morgan, D. Mehta and D. J. Wales, *Phys. Chem. Chem. Phys.*, 2017, **19**, 25498–25508.
90 H. Eyring, *Chem. Rev.*, 1935, **17**, 65.
91 M. G. Evans and M. Polanyi, *Trans. Faraday Soc.*, 1935, **31**, 875.
92 S. A. Trygubenko and D. J. Wales, *Mol. Phys.*, 2006, **104**, 1497–1507.
93 S. A. Trygubenko and D. J. Wales, *J. Chem. Phys.*, 2006, **124**, 234110.
94 A. Banerjee and D. J. Wales, *Phys. Condens. Matter.*, 2021, **34**, 034004.

95 D. J. Sharpe and D. J. Wales, *J. Chem. Phys.*, 2020, **153**, 024121.
96 D. J. Wales, *J. Phys. Chem. Lett.*, 2022, **13**, 6349–6358.
97 D. J. Sharpe and D. J. Wales, *J. Chem. Phys.*, 2021, **155**, 140901.
98 P. G. Mezey, *Potential Energy Hypersurfaces*, Elsevier, Amsterdam, 1987.
99 S. Raschka, *arXiv*, 2018, preprint, arXiv:1811.12808, DOI: 10.48550/arXiv.1811.12808.
100 P. Chaudhari, A. Choromanska, S. Soatto, Y. LeCun, C. Baldassi, C. Borgs, J. Chayes, L. Sagun and R. Zecchina, *J. Stat. Mech.: Theory Exp.*, 2019, **2019**, 124018.
101 P. Foret, A. Kleiner, H. Mobahi and B. Neyshabur, *arXiv*, 2020, preprint, arXiv:2010.01412, DOI: 10.48550/arXiv.2010.01412.
102 M. Andriushchenko and N. Flammarion, *International Conference on Machine Learning*, 2022, pp. 639–668.
103 F. H. Stillinger and T. A. Weber, *J. Stat. Phys.*, 1988, **52**, 1429–1445.
104 S. Hochreiter and J. Schmidhuber, *Neural Comput.*, 1997, **9**, 1–42.
105 G. E. Hinton and D. Van Camp, *Proceedings of the sixth annual conference on Computational learning theory*, 1993, pp. 5–13.
106 Y. Zhang, A. M. Saxe, M. S. Advani and A. A. Lee, *Mol. Phys.*, 2018, **116**, 3214–3223.
107 Y. Yang, C. Rashtchian, H. Zhang, R. R. Salakhutdinov and K. Chaudhuri, *Advances in neural information processing systems*, 2020, vol. 33, pp. 8588–8601.
108 M. S. Pepe, T. Cai and G. Longton, *Biometrics*, 2006, **62**, 221–229.
109 S. Hashem, *Neural Networks*, 1997, **10**, 599–614.
110 H. Jin and Y. Lu, *Stat. Probab. Lett.*, 2009, **79**, 2321–2327.
111 L. Breiman, *Mach. Learn.*, 1996, **24**, 123–140.
112 J. Azimi, A. Fern and X. Fern, *Advances in Neural Information Processing Systems*, 2010, vol. 23.
113 J. Gonazález, Z. Dai, P. Hennig and N. Lawrence, *Artificial Intell. Stat.*, 2016, pp. 648–657.
114 M. Groves and E. O. Pyzer-Knapp, *arXiv*, 2018, preprint, arXiv:1806.01159v2, DOI: 10.48550/arXiv.1806.01159.
115 J. Wilson, V. Borovitskiy, A. Terenin, P. Mostowsky and M. Deisenroth, *Int. Conf. Mach. Learn.*, 2020, pp. 10292–10302.
116 M. Adachi, S. Kayakawa, S. Hamid, M. J. rgensen, H. Oberhauser and M. A. Obsourne, *arXiv*, 2023, preprint, arxiv:2301.11832, DOI: 10.48550/arXiv.2301.11832.
117 M. Galar, A. Fernandez, E. Barrenechea, H. Bustince and F. Herrera, *IEEE Trans. Syst. Man Cybern.: Syst. C*, 2011, **42**, 463–484.
118 M. Zhang, *Pattern Recognit.*, 2022, **124**, 108428.
119 D. Alvarez-Melis and T. S. Jaakkola, *arXiv*, 2018, preprint, arXiv:1806.08049, DOI: 10.48550/arXiv.1806.08049.
120 S. Srinivas and F. Fleuret, *arXiv*, 2020, preprint, arXiv:2006.09128, DOI: 10.48550/arXiv.2006.09128.
121 K. Röder, G. Stirnemann, A. Dock-Bregeon, D. J. Wales and S. Pasquali, *Nucleic Acids Res.*, 2019, 373–389.
122 K. Röder and D. J. Wales, *Front. Mol. Biosci.*, 2022, **9**, 820792.
123 M. P. Niroomand and D. J. Wales, *ICLR 2023 Workshop on Physics for Machine Learning*, 2023.
124 J. C. Dunn, *J. Cybersecur.*, 1974, **4**, 95–104.
125 D. L. Davies and D. W. Bouldin, *IEEE Trans. Pattern Anal. Mach. Intell.*, 1979, **1**, 224–227.
126 P. J. Rousseeuw, *Comput. Appl. Math.*, 1987, **20**, 53–65.
127 R. Tibshirani, G. Walther and T. Hastie, *J. R. Stat. Soc. Ser. B Methodol.*, 2001, **63**, 411–423.
128 E. Schubert, *arXiv*, 2023, preprint, arxiv:2212.12189, DOI: 10.48550/arXiv.2212.12189.
129 Y. Wu, L. Dicks and D. J. Wales, *arXiv*, 2023, preprint, arxiv:2305.17279, DOI: 10.48550/arXiv.2305.17279.
130 A. Svensson, J. Dahlin and T. B. Schön, *2015 IEEE 6th International Workshop on Computational Advances in Multi-Sensor Adaptive Processing*, CAMSAP, 2015, pp. 477–480.
131 R. M. Neal, *arXiv*, 1997, preprint, arxiv:physics/9701026, DOI: 10.48550/arXiv.physics/9701026.
132 C. K. Williams and C. E. Rasmussen, *Neural Information Processing Systems*, NIPS, 1996.
133 A. Garbuno-Inigo, F. A. DiazDelaO and K. Zuev, *Comput. Stat. Data Anal.*, 2016, **103**, 367–383.
134 P. Del Moral, A. Doucet and A. Jasra, *J. R. Stat. Soc. Ser. B Methodol.*, 2006, **68**, 411–436.
135 M. A. Osborne, S. J. Roberts, A. Rogers, S. D. Ramchurn and N. R. Jennings, *2008 International Conference on Information Processing in Sensor Networks (ipsn 2008)*, 2008, pp. 109–120.
136 Y. Saatçi, R. D. Turner and C. E. Rasmussen, *ICML-10*, 2010, pp. 927–934.
137 D. K. Agarwal and A. E. Gelfand, *Stat. Comput.*, 2005, **15**, 61–69.
138 D. Petelin, M. Gasperin and V. Smídl, *IFAC Proc. Vol.*, 2014, **47**, 5011–5016.
139 J. M. Hernández-Lobato, M. W. Hoffman and Z. Ghahramani, *Advances in neural information processing systems*, 2014, vol. 27.
140 G. D. Ath, R. M. Everson and J. E. Fieldsend, *Proc. Genetic. Evol. Comput. Conf. Companion*, 2021, pp. 1860–1869.
141 Y. Saikai, *arXiv*, 2022, preprint, arxiv:2208.13960, DOI: 10.48550/arXiv.2208.13960.
142 V. Lalchand and C. E. Rasmussen, *Proc. Mach. Learn. Res.*, 2020, 1–12.
143 F. Leibfried, V. Dutordoir, S. T. John and N. Durrange, *arXiv*, 2020, preprint, arxiv:2012.13962, DOI: 10.48550/arXiv.2012.13962.